SciEn
Journal of Engineering Advancements Vol. 03(01) 2022, pp 023-028 https://doi.org/10.38032/jea.2022.01.004

Mechanical and Energy Absorption Performance of Expanded Perlite Foam-filled Steel Tubes

Sadman Shahriar, Md. Arifuzzaman, Pranto Karua*

Department of Mechanical Engineering, Khulna University of Engineering & Technology, Khulna 9203, BANGLADESH

Received: March 13, 2022, Revised: March 22, 2022, Accepted: March 22, 2022, Available Online: March 24, 2022

ABSTRACT

The main objective of this research is to manufacture expanded perlite (EP) foam-filled stainless steel tubes for energy absorption application and to investigate their physical and compressive behavior. Foam-filled steel tubes (FFT) were manufactured by consolidating expanded perlite/sodium silicate composite foam inside the tube. The EP particles of size 5-6 mm were taken for manufacturing FFTs. Two different sodium silicate solution to water (S/W) ratios and three compaction ratios (CR) were the manufacturing parameters of the foams. The manufactured FFTs were characterized for density, yield stress, plateau stress, energy absorption, and energy absorption efficiency. The compression test results showed that the foam filling improved the compressive properties and energy absorption ability of the steel tube significantly. The failure analysis along with the stress-strain curves was also conducted. The change in failure mechanism is found to be the reason for high energy absorption and energy absorption efficiency for high-density foam-filled tubes.

Keywords: Expanded Perlite, Composite Foam, Foam Filled Tube, Energy Absorption Capacity.

1 Introduction

In recent years, the main concern of motor vehicles manufacturers is creating safer vehicles with minimum damage when there is an accidental impact [1]. It is necessary to provide an energy-absorbing structure at the front bumper to minimize the damage due to impact. To meet this criterion, different types of empty and composites foam tubes are used as energy-absorbing elements in the design of the vehicle e.g. crash box and anti-intrusion bars [2]. The empty profiles absorb the impact energy of crash at a very low force level and reduce the damage to the vehicle and are considered as mostly inefficient while kept under bending conditions as a high amount of deformation occurs in a small hinge. The crashworthiness of empty tubes under compressive loading conditions was investigated by many researchers [3]. The researches indicate that the energy absorption capacity of such tubes is limited. It is found that simply increasing the thickness of tube walls or implementing double walls tubes can result in increasing specific energy absorption [4]. But a great change is observed using foam filler material inside the tubes and investigations have been done depending on foam fillers to enhance the energy absorption and mechanical properties of thin-walled tubes. Studies have shown that the damping level of different components can be increased up to five times by inserting metallic foams in them [5]. Applications of such foam-filled tubes include anti-intrusion bars [6], crash boxes [7], frame of coach structures [8], or bumpers in the car industry [9]. Nonetheless, the non-metallic foam fillers may also be used for manufacturing foam filled-tubes for energy absorption applications where the cost and the lightweight are the main concerns. For example, Aktay, et al. [10] and Toksoy and Guden [11] studied polystyrene foam-filled aluminum tubes while Meguid, et al. [12] and Alia, et al. [13] investigated PVC foam-filled steel and aluminum tubes to observe the crashing and energy absorption behavior. Expanded perlite composite foams are newly developed low-cost materials which can be manufactured using expanded perlite particles with various binders including sodium silicate solution [14], starch [15], epoxy [16], recycled polystyrene [17], sodium silicate solution with corn starch [18]. These low-cost composite foams may be a good alternative to be used as filler for steel tubes to enhance the mechanical and energy absorption capacity of the filled tubes.

Therefore, in this work, the expanded perlite/sodium silicate foam-filled stainless steel tubes were produced through a cost-effective compaction process. The quasi-static compressive test was conducted on the hollow and foam-filled tubes for characterization. The compressive properties, energy absorption per unit volume, and energy absorption efficiency were investigated based on the manufacturing parameters and the density to find out the effectiveness of expanded perlite/sodium silicate foam filling in the steel tube.

Fig. 1 Expanded perlite particles (5-6 mm)

2 Materials and Methodology

2.1 Materials

2.1.1 Expanded Perlite

Expanded perlite (EP) was collected from China and separated into different size groups using sieves and particles of sizes 5-6 mm were selected for this work (see Fig. 1). The measured bulk density of the particles is 0.073 g/cm^3.

*Corresponding Author Email Address: arif48@me.kuet.ac.bd

2.1.2 Sodium Silicate Solution and Stainless Steel Tube

Sodium silicate solution (SSS) with weight ratio (SiO_2/Na_2O) 3.22 and a density of 1.38 g/cm^3 was diluted using drinking water and used as a binder for manufacturing expanded perlite composite foams. Two different SSS to water ratios (1:1 and 2:1 by weight) were considered in this work. Stainless steel (304) welded tubes of 25.4 mm outside diameter and 0.4 mm thickness were used as shown in Fig. 2. The measured tube bulk density is 0.567 g/cm^3.

Fig. 2 Hollow stainless steel tube (Diameter = 25.4 mm and thickness = 0.4 mm)

2.2 Specimen Preparation

A steel tube was taken and one side of it was covered by a polymer net so that the SSS can pass leaving wet EP particles trapped inside the tube. The tube was filled with the required amount of EP and soaked in the diluted SSS for 2 minutes for proper wetting of the particles. The tube with wet EP particles was taken out of the binder and the excess binder was drained out of the tube. The tube was then taken to the universal testing machine and the wet EP particles inside the tube were compacted using a plunger of a diameter slightly less than the internal diameter of the tube until the final height became 40 mm. The particles remained compacted for about 5 minutes and there was an insignificant spring back. The particles were compacted for three values of compaction ratios (e.g. 2.5, 3.0, and 3.5). Note that, the compaction ratio is the ratio of the height of the loose particle column to the final height after compaction. The specimens were then kept inside an oven at 110°C for curing until the weight loss became constant. The hollow part of the tube with no particles was cut by a hand grinder and both sides of the tube were flattened using a CNC lathe. The specimens may be identified as S_X_Y where 'S' for sample, the number in place of X and Y indicates SSS/Water (S/W) ratio and compaction ratio (CR).

2.3 Mechanical Testing

The uniaxial compression test was conducted on a Universal Testing Machine (Model – Controls 50-C10B/PR) with a loading rate (5 N/s) to investigate the compressive and energy absorption behavior. Four samples for each configuration have been tested.

3 Results and Discussion

3.1 Physical Properties

The mass fractions of constituents and densities of the prepared composites are given in Table 1. Filled tube and foam density are plotted as a function of compaction ratio for two S/W ratios in Fig. 3. Both foam and filled tube density increased linearly with increasing compaction ratio for both binder contents. The least-square lines and R^2 values are also shown in Fig. 3. High linearity is represented by higher R^2 values. The density is higher for a high S/W ratio for all compaction ratios because the EP particles were exposed to a high concentration of sodium silicate during manufacturing. The high value of the mass fraction of sodium silicate in foam (see Table 1) is also seen for a high S/W ratio because of the same reason.

Table 1 Mass fractions and density of the foam-filled steel tube (Average values calculated from three specimens are given in the table).

Sample No.	Mass fraction of EP in foam (%)	Mass fraction of sodium silicate in foam (%)	Mass fraction of foam	Mass fraction of steel tube	Filled tube density (g/cm^3)	Foam density (g/cm^3)
S_1_2.5	72.53	27.47	31.56	68.44	0.83	0.27
S_1_3.0	70.20	29.80	37.17	62.84	0.90	0.35
S_1_3.5	64.24	35.76	41.66	58.34	0.98	0.43
S_2_2.5	44.90	55.11	42.32	57.68	0.99	0.44
S_2_3.0	46.54	53.47	46.90	53.11	1.07	0.52
S_2_3.5	47.58	52.42	49.11	50.90	1.12	0.58

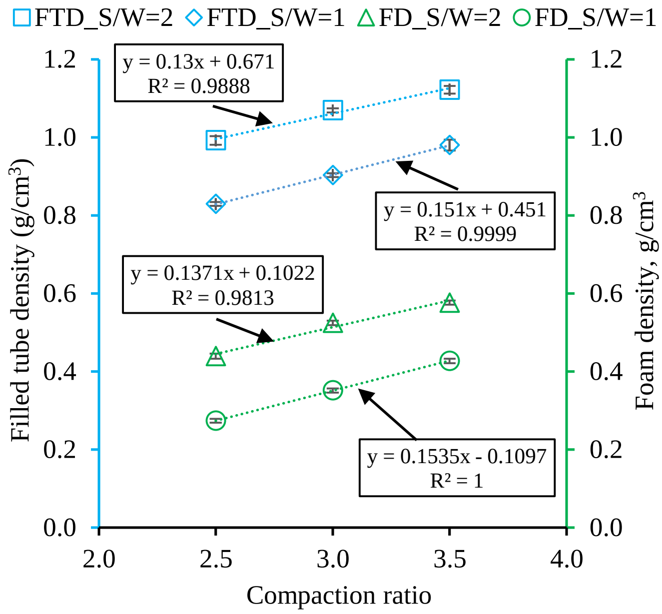

Fig. 3 Filled tube density and foam density as a function of CRs for both S/W ratios. Standard deviations calculated from four specimens are given as error bars.

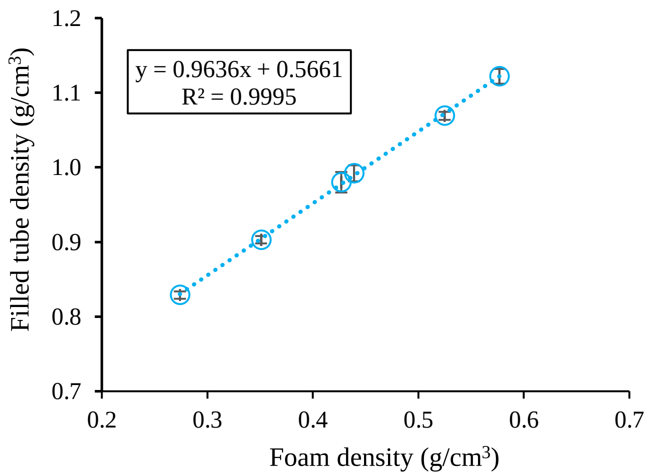

Fig. 4 Filled tube density as a function of foam density

In Fig. 4, the filled tube density is plotted as a function of foam density irrespective of S/W ratios. It is seen that the filled tube density increased linearly showing a high correlation coefficient with increasing foam density regardless of the S/W ratio and CR.

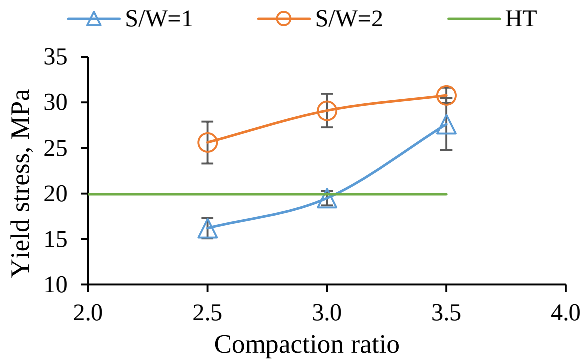

(a)

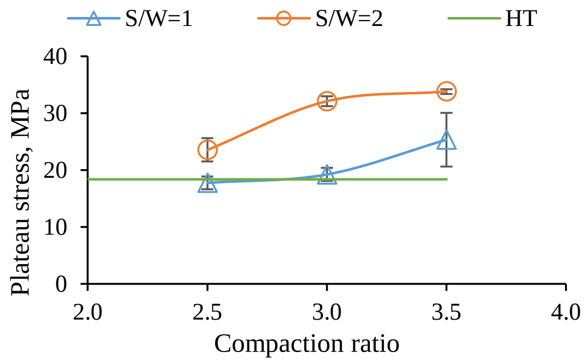

(b)

Fig. 5 Compressive properties of the HT and tubes filled with EP/SSS foam for different CRs for S/W ratios: (a) Yield stress; and (b) Plateau stress (20-40% strain).

3.2 Compressive Properties

3.2.1 Effect of Foam Manufacturing Parameters on Compressive Properties of Foam-filled Tubes (FFT)

In Fig. 5, the compressive properties are plotted as a function of CR for both S/W ratios. It is seen from Fig. 5(a) that the yield stress (YS) increases consistently with the increasing CR for both S/W ratios. The YSs for S/W ratio = 1 at compaction ratios 2.5 and 3.0 appear to be lower than that of the hollow tube (HT). There may be two reasons for this to occur i. e. the prestressing of the tube during the compaction of perlite composite foam inside the tube and the load-bearing capacity of the foam is not sufficient to compensate for the prestressing of the tube. Nonetheless, for the S/W ratio = 1 and CR = 3.5, the YS is higher than that of the HT because the load-bearing capacity of the foam is now sufficient to compensate for the prestressing of the tube. On the other hand, for S/W ratio = 2, all FFTs show higher YS when compared with the YS of HT because of the higher binder content in the foam. It should be noted that the high compaction ratio and high binder content increases the compressive strength of the perlite/sodium silicate foams [14]. The plateau stress (PS) is calculated by averaging the stress from 20% strain to 40 % strain and plotted as a function of CR in Fig. 5(b). It is seen that the PS also increases with increasing compaction ratio for both S/W ratios. The plateau stress for S/W ratio = 1 for CR = 2.0 and 2.5 are very close to the PS of the HT because of the same reason described for YS. Again the PS for S/W ratio = 2 is higher than the HT due to the higher strength of the foams.

Fig. 6 shows the energy absorption (EA) up to 40% strain and the energy absorption efficiency (EAE) at 40% strain of the HT and FFTs as a function of CRs for both S/W ratios. The EA increases consistently with increasing CR for both S/W ratios. The EA is significantly higher in the FFTs as compared to the HT [see Fig. 6(a)] except for the FFT with the foam made of S/W ratio = 2.5 and CR = 2.5. The FFTs with low S/W ratios and low CRs (i. e. S/W=1 with CR=2.5 and 3.0; S/W=2 with CR=2.5) show less EAE and FFTs with high S/W ratios and high CRs (i. e. S/W=1 with CR=3.5; S/W=2 with CR = 2.5 and 3.0) show higher EAE compared to the EAE of the HT [see Fig. 6(b)]. The less EAE for some FFTs is attributed to the low load-bearing capacity as well as the prestressing of the tube during FFT manufacturing.

Therefore, it is seen that the manufacturing parameters of perlite/sodium silicate composites i.e. S/W ratio and CR play an important role in the improvement of mechanical properties of FFTs.

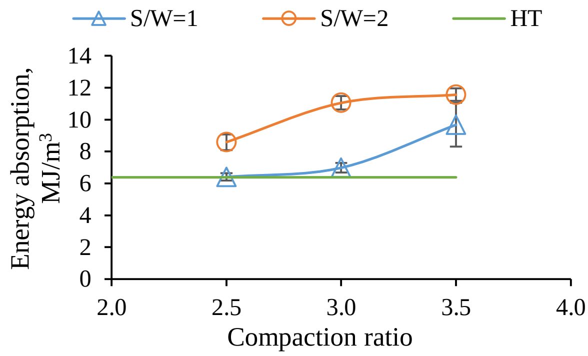

(a)

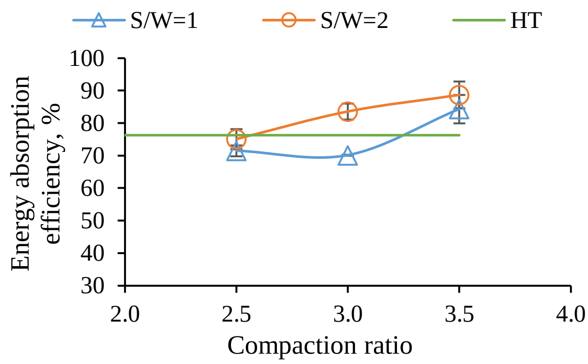

(b)

Fig. 6 (a) Energy absorption per unit volume up to 40% strain and (b) Energy absorption efficiency at 40% strain as functions of CR for both S/W ratios.

3.2.2 Effect of Density on Compressive Properties of the Foam-filled Tubes

In Fig. 7, the YS and PS are plotted as a function of tube density for both HT and FFTs. Both the YS and PS increased highly linearly with increasing the density of the tube as indicated by the high R^2 values. The change in the density of the FFTs is due to the change in the foam density inside the tube because the steel tube size and material are the same for all FFTs. Therefore it is the foam density that caused the increase in both

YS and PS of the FFTs. So, the density of the foam inside the FFTs is highly responsible for the improvement of the compressive properties of the FFTs. The EA and EAE are plotted as a function of tube density in Fig. 8. It is seen that the EA increases linearly with increasing density with a high R^2 value. Although the EAE increases with increasing tube density, the linearity is not high as indicated by the low R^2 value.

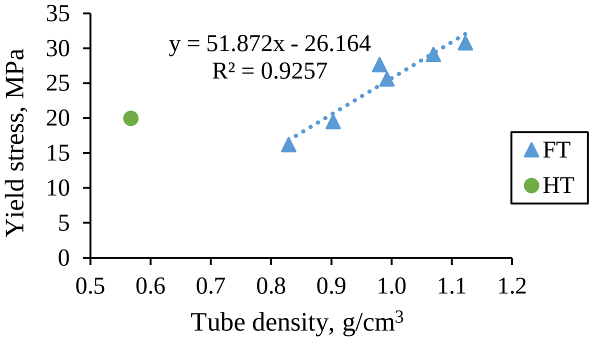

(a)

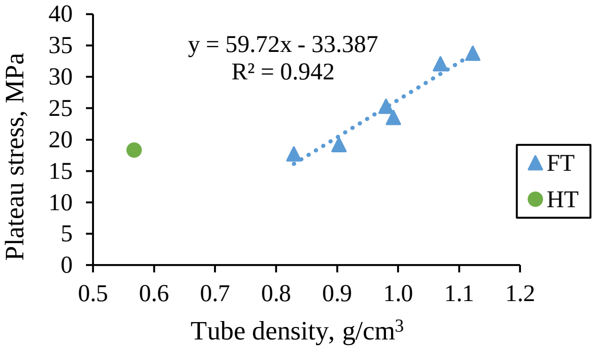

(b)

Fig. 7 Compressive properties of the tubes with the variation of tube density: (a) Yield stress; and (b) Plateau stress (20-40% strain).

From the above results, it can be said that the compressive properties of the FFTs improved significantly when the density of the foam inside the tube is increased as compared to the HT. The percentage increase in YS, PS, EA, and EAE in the highest density FFTs are seen to be 54.49%, 83.84%, 81.63%, and 16.32% respectively compared with the HT. The improvements in mechanical properties and energy absorption occurred with a cost of only an 8.34% decrease in specific energy absorption.

The variation of EAE of the FFTs and HT with strain is shown in Fig. 9. In general, it appears that after the peak stress is reached, the EAE increases with increasing strain for HT and FFTs. It can be seen that the EAE is consistently higher for FFTs filled with perlite foam with CR = 3.0 and 3.5 when compared with EAE of HT throughout the range of strain studied [see Fig. 9(a)]. Though the EAE of S_1_3.0 coincides with HT's EAE, it remains higher for S_1_3.5 than HT's EAE. For samples made of S/W ratio = 2, FFTs show higher EAE compared with HTs for the whole strain range after the peak stress (see Fig. 10) is reached. Therefore, the perlite foam filling has a significant impact in improving the energy absorption efficiency of the tube.

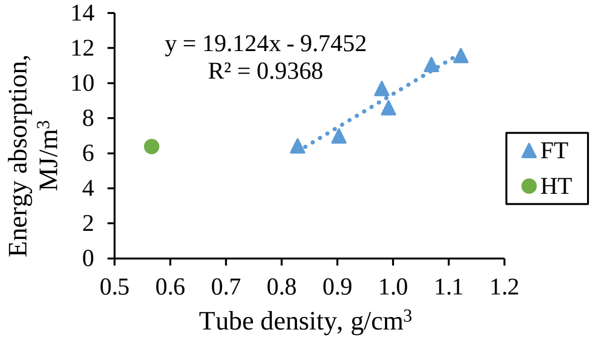

(a)

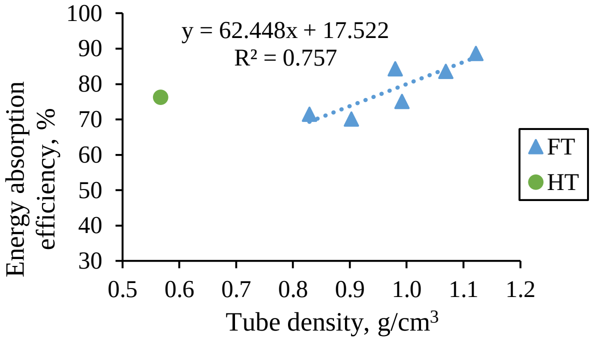

(b)

Fig. 8 (a) Energy absorption per unit volume up to 40% strain and (b) Energy absorption efficiency at 40% strain as a function of tube density.

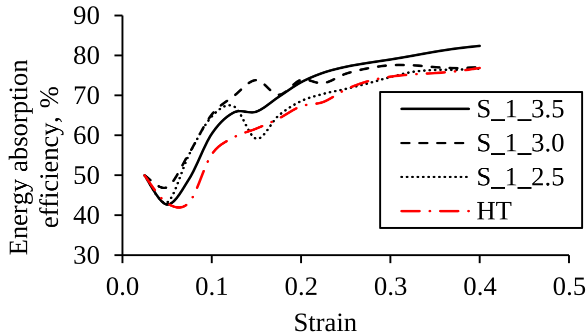

(a)

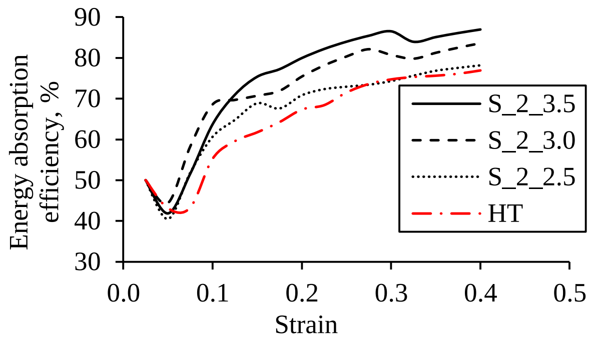

(b)

Fig. 9 Variation of energy absorption efficiency with strain for (a) S/W ratio = 1 and (b) S/W ratio = 2.

3.2.3 Effective Stress-Strain Curves and Failure Analysis

The effective stress versus strain curves for the HT and FFTs are shown in Fig. 10. Stress increases linearly with increasing strain up to a peak (i. e. yield point). After that, the curve for the hollow tube shows two peaks for the range of strain studied. Each peak is associated with each three-fold buckling failure of the tube due to compression as shown in Fig. 11(a). Specimen with S/W ratio = 1 and CR = 2.5 shows three peaks and CR = 3.0 shows two peaks in their respective stress-strain curves but for the specimen with S/W ratio = 1 and CR = 3.5, the curve shows a single peak and then a plateau in the stress-strain curve. However, the failure for the HT is three-fold buckling and for the FFTs with the S/W ratio = 1 consists of a single ring formation and then three-fold buckling as shown in Fig. 11(c) – (f).

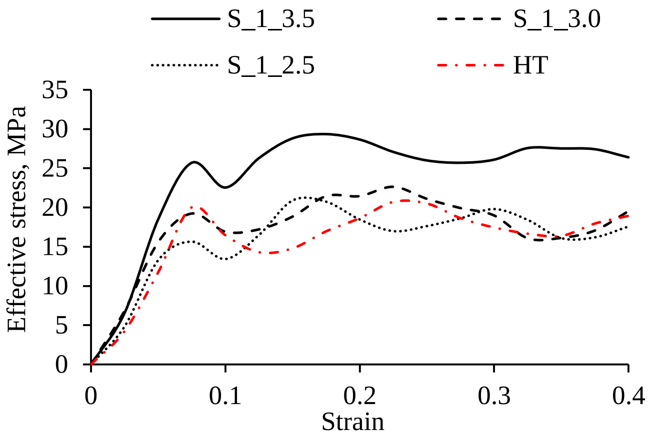

(a)

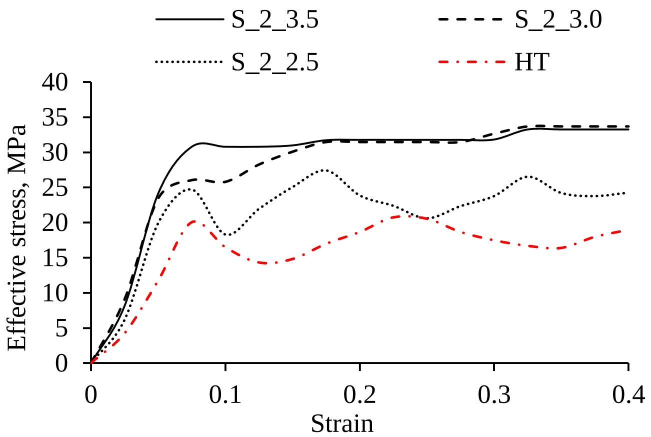

(b)

Fig. 10 Effective stress-strain curves for (a) S/W ratio = 1 and (b) S/W ratio = 2.

On the other hand, the stress-strain curve for S/W ratio = 2, the FFT with CR = 2.5 shows three peaks instead of two peaks for HT although the location of the peak in the stress-strain curve is different. In this case, the failure of the specimen is similar to the FFTs for S/W ratio = 1. For S/W ratio = 2 and CRs = 3.0 and 3.5, the stress-strain curves do not show any peak rather a plateau [see Fig. 11(g)] is seen for the strain range studied. The three-fold buckling failure is eliminated and the failure occurred by the formation of rings (concertina) as seen in Fig. 11(h) and (i). The change in failure mode is the reason for the high energy absorption and energy absorption efficiency of the high-density foam-filled tubes.

Fig. 11 (a) Hollow tube; (b) Foam filled tube; (c) Crashed hollow tube; (d) - (i) Some photographs of the crashed FFT specimens after compression tests made of S/W ratio = 1 and S/W ratio = 2 for various compaction ratios.

4 Conclusion

The work is focused on the development and characterization of perlite foam-filled steel tubes for energy absorption application. The findings of the research can be summarized as:

- The compressive properties, energy absorption, and energy absorption efficiency of the foam-filled tubes significantly depend on the foam manufacturing parameters such as binder content and compaction ratio.
- The percentage increase in yield stress, plateau stress, and energy absorption in the highest density foam-filled tube is found to be 54.49%, 83.84%, and 81.63% respectively compared with those of the hollow tube. The improvements in mechanical properties and energy absorption occurred with a cost of only an 8.34% decrease in specific energy absorption.
- The energy absorption efficiency is found to be increasing with increasing strain and EAE is higher than that of the hollow tube throughout the range of strain studied except for the low-density foams.
- For the high-density foam-filled tubes, the failure mechanism is changed from three-fold buckling to the formation concertina which is the reason for the high energy absorption capacity of those foam-filled tubes.

Nomenclature

Parameters	Acronyms
Expanded perlite	EP
Sodium silicate solution	SSS
Foam-filled tube	FFT
Hollow tube	HT
Yield stress	YS
Plateau stress	PS
Energy absorption	EA
Energy absorption efficiency	EAE
Sodium silicate solution to water ratio	S/W ratio
Compaction ratio	CR

Acknowledgements

The authors acknowledge the financial support for this work from Khulna University of Engineering & Technology.

References

[1] Xiao, Z., Fang, J., Sun, G. and Li, Q., 2015. Crashworthiness design for functionally graded foam-filled bumper beam. *Advances in Engineering Software*, *85*, pp.81-95.

[2] Zarei, H.R. and Kröger, M., 2007. Crashworthiness optimization of empty and filled aluminum crash boxes. *International Journal of Crashworthiness*, *12*(3), pp.255-264.

[3] Abramowicz, W., 2003. Thin-walled structures as impact energy absorbers. *Thin-walled structures*, *41*(2-3), pp.91-107.

[4] Kavi, H., Toksoy, A.K. and Guden, M., 2006. Predicting energy absorption in a foam-filled thin-walled aluminum tube based on experimentally determined strengthening coefficient. *Materials & design*, *27*(4), pp.263-269.

[5] Strano, M., Marra, A., Mussi, V., Goletti, M. and Bocher, P., 2015. Endurance of damping properties of foam-filled tubes. *Materials*, *8*(7), pp.4061-4079.

[6] Strano, M., Villa, A. and Mussi, V., 2013. Design and manufacturing of anti-intrusion bars made of aluminium foam filled tubes. *International Journal of Material Forming*, *6*(1), pp.153-164.

[7] Zarei, H.R. and Kröger, M., 2008. Optimization of the foam-filled aluminum tubes for crush box application. *Thin-walled Structures*, *46*(2), pp.214-221.

[8] Cazzola, G.J., Alcalá Fazio, E. and Izquierdo, F.A., 2013. Study of the bending response of metal foam-filled beams applied to enhance the rollover behaviour of coach structures. *International Journal of Crashworthiness*, *18*(6), pp.620-632.

[9] Ahmad, Z. and Thambiratnam, D.P., 2009. Application of foam-filled conical tubes in enhancing the crashworthiness performance of vehicle protective structures. *International Journal of Crashworthiness*, *14*(4), pp.349-363.

[10] Aktay, L., Toksoy, A.K. and Güden, M., 2006. Quasi-static axial crushing of extruded polystyrene foam-filled thin-walled aluminum tubes: experimental and numerical analysis. *Materials & Design*, *27*(7), pp.556-565.

[11] Toksoy, A.K. and Güden, M., 2005. The strengthening effect of polystyrene foam filling in aluminum thin-walled cylindrical tubes. *Thin-walled structures*, *43*(2), pp.333-350.

[12] Meguid, S.A., Attia, M.S. and Monfort, A., 2004. On the crush behaviour of ultralight foam-filled structures. *Materials & Design*, *25*(3), pp.183-189.

[13] Alia, R.A., Guan, Z., Jones, N. and Cantwell, W.J., 2015. The energy-absorption characteristics of metal tube-reinforced polymer foams. *Journal of Sandwich Structures & Materials*, *17*(1), pp.74-94.

[14] Arifuzzaman, M.D. and Kim, H.S., 2014, December. Development of new perlite/sodium silicate composites. In *International Conference on Mechanical, Industrial and Energy Engineering (ICMIEE), Khulna University of Engineering & Technology, Khulna, Bangladesh*.

[15] Shastri, D. and Kim, H.S., 2014. A new consolidation process for expanded perlite particles. *Construction and Building Materials*, *60*, pp.1-7.

[16] Allameh-Haery, H., Kisi, E. and Fiedler, T., 2017. Novel cellular perlite–epoxy foams: Effect of density on mechanical properties. *Journal of Cellular Plastics*, *53*(4), pp.425-442.

[17] Al Abir, A., Faruk, M.O. and Arifuzzaman, M. 2021, December. Novel Expanded Perlite Based Composite using Recycled Expanded Polystyrene for Building Material Applications. In *International Conference on Mechanical, Industrial and Energy Engineering (ICMIEE), Khulna University of Engineering & Technology, Khulna, Bangladesh*.

[18] Adhikary, P., Arifuzzaman, M. and Kabir, E., 2020. Compressive properties of expanded perlite based particulate composite for the application in building insulation Board. *Journal of Engineering Advancements*, *1*(1), pp.01-05.